


 Cite this: *Chem. Sci.*, 2019, **10**, 7484

All publication charges for this article have been paid for by the Royal Society of Chemistry

Received 5th June 2019

Accepted 12th July 2019

DOI: 10.1039/c9sc02743b

[rsc.li/chemical-science](http://rsc.li/chemical-science)

## A review of biomass materials for advanced lithium–sulfur batteries

Huadong Yuan,<sup>†</sup> Tiefeng Liu,<sup>†</sup> Yujing Liu, Jianwei Nai, Yao Wang, Wenkui Zhang and Xinyong Tao  \*

High energy density and low cost make lithium–sulfur (Li–S) batteries famous in the field of energy storage systems. However, the advancement of Li–S batteries is evidently hindered by the notorious shuttle effect and other issues that occur in sulfur cathodes during cycles. Among various strategies applied in Li–S batteries, using biomass-derived materials is more promising due to their outstanding advantages including strong physical and chemical adsorptions as well as abundant sources, low cost, and environmental friendliness. This review summarizes the recent progress of biomass-derived materials in Li–S batteries. By focusing on the aspects of carbon hosts, separator materials, bio-polymer binders, and all-solid-state electrolytes, the authors aim to shed light on the rational design and utilization of biomass-derived materials in Li–S batteries with high energy density and long cycle lifespan. Perspectives regarding future research opportunities in biomass-derived materials for Li–S batteries are also discussed.

## 1 Introduction

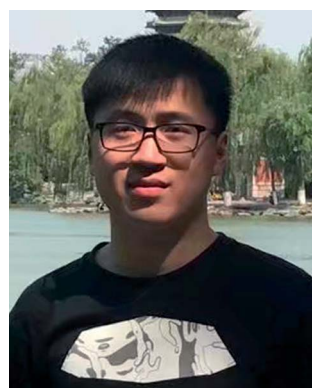
The demand for energy storage technologies continues to increase due to their future applications in electric vehicles and smart grids. Lithium-ion batteries (LIBs) based on an intercalation mechanism feature the highest energy density among commercially viable energy storage technologies, but are approaching the limitation of theoretical energy density.<sup>1–5</sup> Therefore, a new energy storage system with higher energy density is urgently required. Lithium–sulfur (Li–S) batteries, coupled with a sulfur cathode and a lithium metal anode, have

attracted increasing attention due to their high energy density (around 2600 W h kg<sup>–1</sup>). The practically viable energy density of Li–S batteries is still 2–3 times higher than that of the state-of-the-art commercial LIBs.<sup>6–10</sup> Unfortunately, the real-world applications of Li–S batteries are restricted by the low conductivity of sulfur and discharge products (Li<sub>2</sub>S/Li<sub>2</sub>S<sub>2</sub>), high volume expansion of sulfur during cycles, serious shuttle effect originating from the dissolved lithium polysulfides (LiPSs) in the electrolyte, and irreversible Li<sub>2</sub>S/Li<sub>2</sub>S<sub>2</sub> deposition and phase conversion.<sup>9,11–13</sup>

So far, these challenges have driven intensive research on potential solutions including novel strategies and materials. Strategies to suppress polysulfide shuttling and stabilize cycle life can be divided into constructing polar sulfur hosts,<sup>14–19</sup> developing multifunctional separators,<sup>20–22</sup> introducing all-solid-state

Department of Materials Science and Engineering, Zhejiang University of Technology, Hangzhou 310014, China. E-mail: tao@zjut.edu.cn

† These authors contributed equally to this work.



*Huadong Yuan received his BS in Materials Science and Engineering from Northeast Forestry University in 2013. He is currently a Ph.D. candidate in the Professor Xinyong Tao group at the Zhejiang University of Technology. His research is now focused on advanced electrode materials for energy storage such as lithium–sulfur batteries, lithium metal anodes, and lithium ion batteries.*



*Tiefeng Liu received his Ph.D. degree from the Harbin Institute of Technology in 2017 and went to work as a postdoctoral researcher at the Guangdong University of Technology. In 2019, he became a member of the Tao Group. His main research interests are focused on green design of lithium/sodium ion batteries.*



electrolytes,<sup>23–25</sup> etc.<sup>26–29</sup> Accordingly, corresponding materials such as graphene, MXenes, nanotubes, functional polymers, porous carbon, metal oxides, sulfides and carbides have been massively developed.<sup>30–36</sup> Among them, bio-materials have a great possibility of enabling commercially viable Li–S batteries due to their advantages of strong physical and chemical adsorptions, low-cost, environmental friendliness, and easy accessibility. Furthermore, naturally moulded biomass-based materials have various morphologies. Hence, the exploration of bio-materials to construct



*Yujing Liu received his bachelor's degree in polymer science in 2011 and Ph.D. degree in polymer science and engineering in 2016 from Zhejiang University, China. He is currently an associate professor in the College of Materials Science and Engineering at the Zhejiang University of Technology. His research interests focus on bioinspired strategies for regulating metallic crystallization for energy storage, such as lithium metal anodes and lithium-ion batteries.*



*research interests focus on controllable synthesis and assembly of transition metal-based nanomaterials for energy storage and conversion.*



*Yao Wang received his Bachelor of Science degree from the Department of Physics in 2011 and Ph.D. degree in Materials Science and Engineering in 2018 from Zhejiang University. In 2019, he joined the College of Materials Science and Engineering at the Zhejiang University of Technology. His interests include 2D materials, ferroelectrics and lithium metal anodes.*

key components for Li–S batteries would be worthwhile considering the potential scale of electrochemical applications.<sup>37–45</sup>

This review aims to provide a comprehensive summary of the recent progress of bio-derived materials for Li–S batteries.<sup>38,46,47</sup> We highlight the representative applications of bio-derived materials in Li–S batteries as the following four parts: carbon hosts, separator materials, bio-polymer binders, and all-solid-state electrolytes. Structural and chemical characterization of bio-materials is briefly surveyed. Finally, we conclude by presenting our perspective and suggestions on the further development of bio-derived materials in Li–S batteries.

## 2 Carbon hosts derived from biomass for storing sulfur

Due to their inherited specific structures, carbon materials derived from biomass (CDB) have attracted great attention as a promising host for storing sulfur.<sup>48,49</sup> Furthermore, the richness of biomass in nature allows a variety of CDBs to be obtained. In this section, the progress of the representative CDBs as a carbon host for sulfur will be summarized and discussed.

Fibrous biomass such as kapok, cotton, and bacterial cellulose with a 3D cross-linked and porous structure is a promising carbon precursor candidate for carbon hosts. Benefiting from the inherited network structure, the resultant carbon host can enable high sulfur loading and fast electron transfer in a sulfur cathode. Employing low-cost and high-yield kapok fibers (KFs) as a carbon precursor, Tao and co-workers developed carbon nanoflakes modified with metal oxides ( $M_xO_y/C$ ,  $M = Al, Ce, La$ ,



*Wenkui Zhang is a professor in the College of Materials Science and Engineering at the Zhejiang University of Technology. He received his Ph.D. degree in 1997 from Zhejiang University. His research interests focus on advanced secondary batteries and energy storage/conversion materials such as lithium-ion batteries, lithium–sulfur batteries, fuel cells, and supercapacitors.*



*Xinyong Tao received his Ph.D. from the School of Materials Science and Engineering at Zhejiang University (2007). He is now a Professor in the College of Materials Science and Engineering at the Zhejiang University of Technology. His main research interest is focused on the design and synthesis of green materials for energy storage such as lithium–sulfur batteries, lithium metal anodes, and lithium-ion batteries.*



Mg, or Ca) *via* a simple carbonization step.<sup>12</sup> A schematic of the fabrication of  $M_xO_y/C$  is illustrated in Fig. 2a. With the help of capillarity, the solution containing a certain metal nitrate is infiltrated into the KFs. Subsequently, scalable carbon nanoflakes decorated with ( $M_xO_y/C$ ) nanoparticles are readily synthesized through a carbonization process. Due to the high surface area of the materials and high capability of metal oxides for trapping polysulfides, the sulfur cathodes can deliver high sulfur utilization and stable cycling performance (Fig. 1).<sup>12</sup>

An additional demonstration of a carbon host for sulfur is carbon cotton, which was applied in Li-S batteries by Manthiram and co-workers.<sup>50</sup> Fig. 2b shows the fabrication procedures of the flexible carbon-cotton cathode, which was synthesized through a simple carbonization step at 900 °C for 6 h under an Ar atmosphere.<sup>50</sup> The obtained carbon cotton has a high surface area ( $805 \text{ m}^2 \text{ g}^{-1}$ ), good porous structure, excellent mechanical strength, and cross-linked conductive network (Fig. 2c). Therefore, an ultrahigh sulfur loading ranging from 30.7 to 61.4  $\text{mg cm}^{-2}$  is successfully achieved *via* a thermal diffusion method.<sup>50</sup> Besides KFs and cotton, other fibrous biomass materials, such as bacterial cellulose, cotton cloth, silk and cobweb, are also considered for carbon hosts.<sup>51,52</sup> These web-like biomass materials with a high surface area are conducive to integrating with sulfur and converting to carbon materials with high conductivity. Furthermore, silk and cobweb can form nitrogen dopants in the obtained carbon materials during the carbonization process, which is favorable for trapping polysulfides and improving sulfur utilization for Li-S batteries.<sup>53</sup>

Multiporous carbon materials derived from biomass are other promising candidates for storing sulfur due to their high surface area and superior physical adsorption for polysulfides. Rice, a staple food for people, is made up of starch. Inspired by

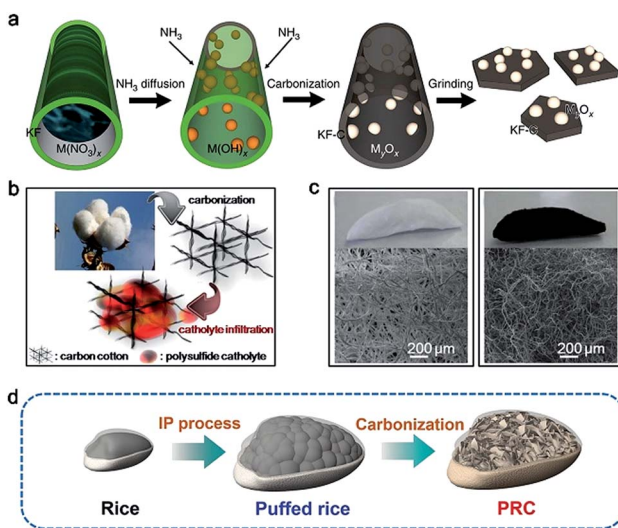


Fig. 2 (a) Fabrication diagram of  $M_xO_y/C$  composites. Reproduced with permission.<sup>12</sup> Copyright 2016, Nature publishing group. (b) Schematic of the fabrication process of carbonized cotton. (c) Digital and SEM images of cotton and carbonized cotton. Reproduced with permission.<sup>50</sup> Copyright 2016, American Chemical Society. (d) Schematic illustration of PRC. Reproduced with permission.<sup>54</sup> Copyright 2017, Wiley-VCH.

the fabrication process of popcorn, Xia *et al.* developed a puffed rice carbon (PRC) material as a sulfur host *via* a one-pot and facile method.<sup>54</sup> As shown in Fig. 2d, the resultant PRC exhibits a 3D microcellular architecture consisting of numerous interconnected carbon nanoflakes with a thickness of 500 nm. In addition, an effective strategy by using  $\text{NiCl}_2$  as the etching agent is used to improve the electrical conductivity and surface area of the carbon host. Rapid puffing fabrication allows Ni nanoparticles to be *in situ* embedded into PRC and the formation of a highly porous structure in PRC/Ni composites. Taking advantage of such a microcellular structure and good distribution of Ni nanoparticles both in the interior and on the surface, the sulfur cathode based on PRC/Ni composites exhibits a high reversible capacity of  $1257 \text{ mA h g}^{-1}$  and stable cycling performance at 0.2C.

In addition to the microcellular structure of PRC, the 3D aligned microchannels of wood for water transportation is also an ideal structure for sulfur loading. The vast space of the aligned microchannels in wood provides internal room for high sulfur loading. Hu and co-workers synthesized a 3D aligned porous carbon matrix using carbonized wood as the framework and reduced graphene oxide (rGO) as the filler (Fig. 3a and b).<sup>55</sup> The rGO is filled inside the microchannels to promote the construction of multiporous and anti-deformation structures in wood channels, which can effectively improve the sulfur mass loading and the electron transport. The shuttling of polysulfides can also be suppressed due to the rich oxygen functional groups on the surface of rGO inside the wood channels. Employing this design, the sulfur cathode with a high sulfur loading of  $7.8 \text{ mg cm}^{-2}$  exhibits a high areal capacity of  $6.7 \text{ mA h cm}^{-2}$  at a current density of  $1.56 \text{ mA cm}^{-2}$ .

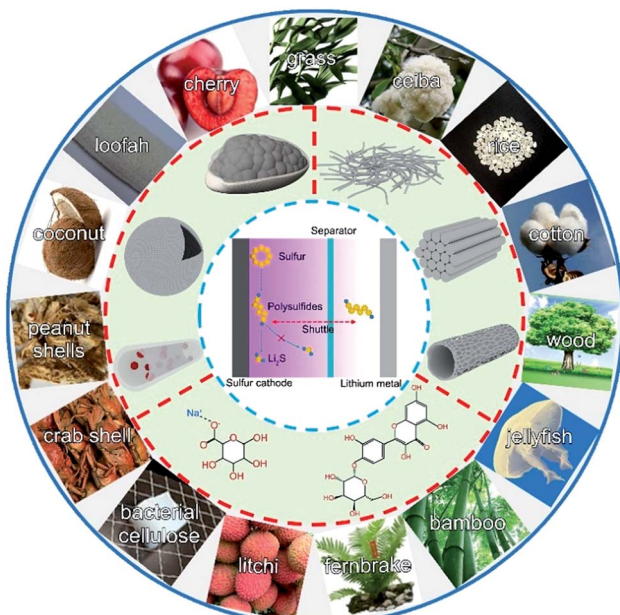


Fig. 1 The schematic diagram of bio-derived materials applied in the Li-S battery system.



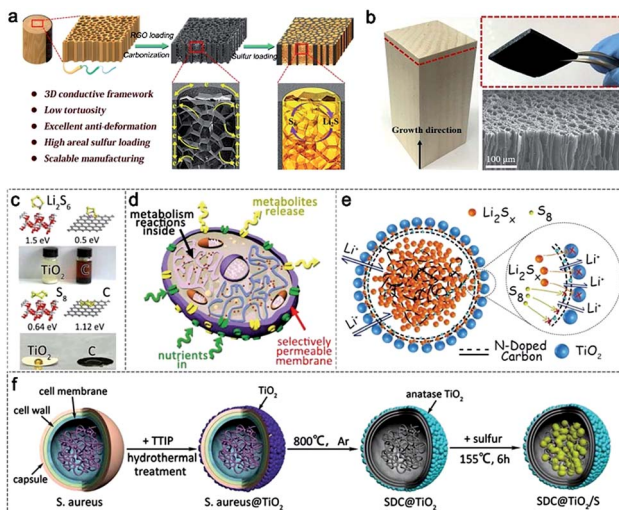


Fig. 3 (a) Schematic illustration of the fabrication process and structure of the S@C-wood composite. (b) Morphological characterization of the C-wood matrix. (a and b) Reproduced with permission.<sup>55</sup> Copyright 2017, American Chemical Society. (c) Binding energy and related adsorption experiments between TiO<sub>2</sub>/carbon and polysulfides. (d) A model of a biological cell. (e) Biomimetic microcapsules. (f) The fabrication procedure of the biomimetic microcapsule confined sulfur cathodes (SDC@TiO<sub>2</sub>/S). (c-f) Reproduced with permission.<sup>57</sup> Copyright 2018, Wiley-VCH.

In addition, wood microfibers with hierarchical and mesoporous structures are other good host materials applied in Li-S batteries,<sup>56</sup> achieving a high sulfur loading of 76 wt%. Besides wood, bacteria, derived from the wastes of the pharmaceutical industry, are other promising precursors for the fabrication of hierarchically porous carbon. The mesoporous structure of the obtained carbon materials increases the utilization of active sulfur materials. For example, Zhang *et al.* developed a kind of uniformly porous carbon using *Staphylococcus aureus* as the precursor.<sup>57</sup> The obtained carbon materials fully inherit the sphere morphology and multiporous structure of *Staphylococcus aureus* (Fig. 3c and d). In addition, modified TiO<sub>2</sub> (Fig. 3e) and N dopants derived from protein after carbonization (Fig. 3f) can be employed for Li-S batteries. As a result, the as-prepared cathodes delivered ultra-stable cycling performance with 0.05% capacity decay per cycle after 1500 cycles at a current density of 1.5 A.

Although multiporous structures are advantageous for storing sulfur, most of the biomass materials have only a few macropore structures. Fortunately, such an issue can be addressed by a simple method at high temperature in an inert atmosphere using activation agents such as KOH, K<sub>2</sub>CO<sub>3</sub>, and ZnCl<sub>2</sub>. Manoj *et al.* reported micro/mesoporous coconut shell carbon with high specific surface areas as a carbon host for Li-S batteries.<sup>62</sup> In addition, Table 1 shows the characterization of other carbon materials obtained from biomass.<sup>58-62</sup> The adjustable structures, eco-friendly fabrication processes, and rich surface chemical groups offer a lot of possibilities for suppressing the shuttle effect and improving sulfur utilization, which crossed the threshold into a new depth of Li-S battery commercialization.

### 3 Bio-derived materials used as separators for preventing the shuttle effect

Besides the wide application of biomass-derived carbon hosts in Li-S batteries, constructing multifunctional separators is considered as another effective method. Not only can the internal charge-transfer resistance of the Li-S cells be reduced, but also the utilization of active materials can be improved. This section will discuss the application of bio-interlayers in Li-S batteries. The reported strategies can be divided into two categories: porous carbon film coating of a commercial separator and freestanding carbon interlayer insertion between the cathode and separator. In general, any bio-derived carbon material can be employed as an active material to coat the commercial separator after the carbonization step. But for freestanding interlayer fabrication, fiber-shaped materials may be more adaptive. In addition, benefitting from the 3D cross-linked structures, the obtained freestanding interlayer is favourable for fast electron transportation in sulfur cathodes. Both porous carbon coated separators and cross-linked interlayers play an important role in preventing the shuttling of polysulfides.

The combination of biomass-derived carbon and a commercialized separator is a simple but effective method to enable a synergistic effect for chemically and physically trapping polysulfides. As illustrated in Fig. 4a, a nitrogen-doped micro-/mesoporous carbon (N-MIMEC) was fabricated using crab shell waste as the source by Huang *et al.*<sup>74</sup> The obtained carbon materials with a channel-like structure possess a large surface area and abundant N dopants, which are often demonstrated for suppressing polysulfide shuttling. And hence, the obtained N-MIMEC-coated separator (Fig. 4b) exhibited many advantages during discharge/charge processes: (i) the micro-/mesopores and rich N-dopants in N-MIMEC provided strong physical and chemical adsorption for polysulfides. (ii) The mesopores in N-MIMEC promote the electrolyte penetration to enable fast diffusion of Li ions. (iii) The as-prepared N-MIMEC layer acts as an upper current collector to improve the electrical conductivity of the electrode. Therefore, enhanced cyclability of Li-S batteries with N-MIMEC-coated separators is readily achieved with a high reversible capacity of 971.3 mA h g<sup>-1</sup> at 0.1C. Other studies have also succeeded in fabricating various porous carbon materials from biomass, such as shrimp shell and sea grass. These carbon materials as adsorption layers are coated on commercial separators, suppressing the shuttle effect of polysulfides. To further block the polysulfides, polar group such as SiO<sub>2</sub> modified bio-carbon materials were fabricated on a commercial separator surface.<sup>75</sup> With the assistance of strong adsorption between the polar group and polysulfides, high sulfur utilization and stable cycling performance are achieved.

3D network bio-fiber materials are other promising interlayer precursor candidates due to their cross-linked framework and rich -OH groups.<sup>76,77</sup> Such a 3D network structure is often made of bacterial cellulose (BC), which naturally consists of interconnected cellulose nanofibers.<sup>78</sup> As shown in Fig. 4d, the fabrication of the BC interlayer was developed by Sun *et al.*<sup>78</sup>



Table 1 Categories, fabrication methods, structures and characteristics of other carbon materials derived from biomass

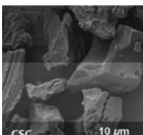
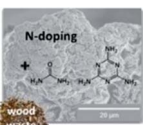
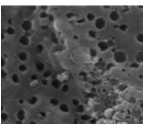
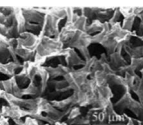
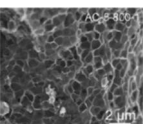
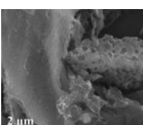
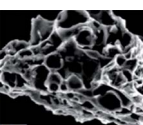
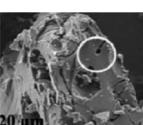
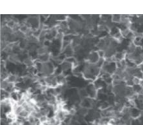
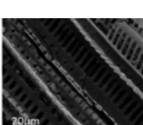
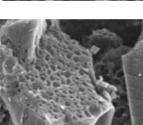
Source	Representative SEM/TEM image	Fabrication method	Surface chemical group
Coconut shell <sup>63,64</sup>		KOH activation	Hydroxyl groups
Wood waste <sup>65</sup>		$K_2CO_3$ activation	N dopants
Walnut shell <sup>66</sup>		KOH activation	Hydroxyl groups
Pomelo peel <sup>67</sup>		KOH activation	Hydroxyl groups
Rapeseed shell <sup>68</sup>		KOH activation	Hydroxyl groups
Seaweed <sup>69</sup>		NaCl activation	N dopants
Coffee waste <sup>70</sup>		$ZnCl_2$ activation	O and N dopants
Cherry pits <sup>71</sup>		$H_3PO_4$ activation	Hydroxyl groups
Bamboo <sup>72</sup>		KOH activation	Hydroxyl groups
<i>Cyclosorus</i> <sup>73</sup>		$KHCO_3$ activation	S and O dopants
Jellyfish <sup>61</sup>		$NH_4H_2PO_4$ activation	N and P dopants



Table 1 (Contd.)

Source	Representative SEM/TEM image	Fabrication method	Surface chemical group
Peanut shell <sup>53</sup>		KOH activation	Hydroxyl groups

Because of the unique interlinked network, the obtained BC interlayer endowed the composites with superior conductivity and a robust framework. More importantly, with the help of the BC interlayer inserted between the sulfur cathode and separator, not only can the excessive accumulation of sulfur be relieved, but also the shuttle effect of polysulfides in the electrolyte can be reduced through a new “guiding” strategy (Fig. 4e).<sup>76–78</sup> The sulfur cathode exhibits a high discharge capacity of 1134 mA h g<sup>-1</sup> at a current density of 200 mA g<sup>-1</sup> after 400 cycles.<sup>78</sup>

Similarly, Rezan Demir-Cakan *et al.* proposed to synthesize freestanding pyrolyzed BC interlayers for suppressing dissolved polysulfides in the electrolyte.<sup>79</sup> During the growth of bacterial cellulose (Fig. 5a), SnO<sub>2</sub> particles were added into the medium of bacteria, leading to the formation of cellulose fibers modified with SnO<sub>2</sub>. Hence, an intimate contact between SnO<sub>2</sub> and bacterial cellulose can be obtained (Fig. 5b). The sulfur cathodes employing the as-prepared SnO<sub>2</sub>@BC interlayer displayed a more stable cycle life than that containing bare pyrolyzed BC as well as without an interlayer.<sup>79</sup>

Besides bacterial cellulose, other cellulose fibers derived from wood and cotton are also investigated as interlayer materials. Cost-effective carbonized cellulose paper (CCP) is a potential interlayer for Li-S batteries.<sup>81</sup> When inserted

between the sulfur cathode and separator, the interlayer significantly improved sulfur utilization and rate performance due to the highly conductive CCP interlayer. Tu and co-workers developed a Ni-embedded porous carbon fiber (PGCF/Ni) interlayer for Li-S batteries through a facile delignification step from bamboo in alkaline solution (Fig. 5c).<sup>82</sup> Metallic Ni nanoparticles are modified to improve the adsorption ability for polysulfides. Due to its attractive properties such as a large surface area, 3D porous structure, and high electrical conductivity, the Li-S batteries employing the functional PGCF/Ni interlayer exhibited improved electrochemical performances (Fig. 5d).

Other biomass with abundant heteroatom dopants after carbonization is another good precursor for interlayer fabrication. Low-cost *Luffa sponge* with abundant sources is the most representative due to the high content of sulfur and oxygen elements. As shown in Fig. 5e, Zhou's group developed a sulfur-doped microporous carbon (SMPC) material *via* a simple step of

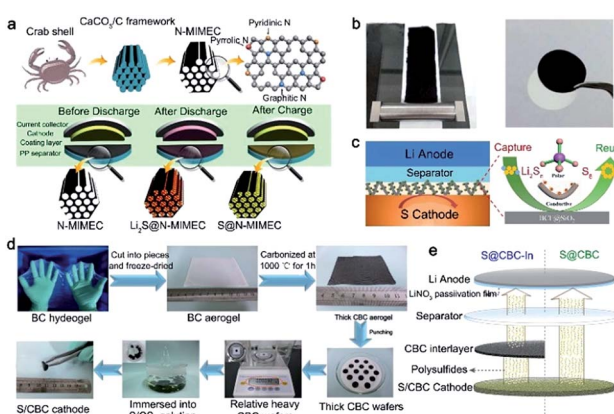


Fig. 4 (a) Fabrication of N-MIMEC using crab shells and the detailed polysulfide suppression mechanisms of the N-MIMEC-coated separator. (b) The digital picture of the N-MIMEC-coated separator. (a and b) Reproduced with permission.<sup>74</sup> Copyright 2017, Royal Society of Chemistry. (c) The LiPS-trapping mechanisms of the BCF@SiO<sub>2</sub> interlayer. (c) Reproduced with permission.<sup>80</sup> Copyright 2018, Elsevier. (d) The procedure for fabricating the freestanding CBC interlayer. (e) Schematic of the working mechanism for Li-S batteries using the CBC interlayer. (d and e) Reproduced with permission.<sup>78</sup> Copyright 2015, Royal Society of Chemistry.

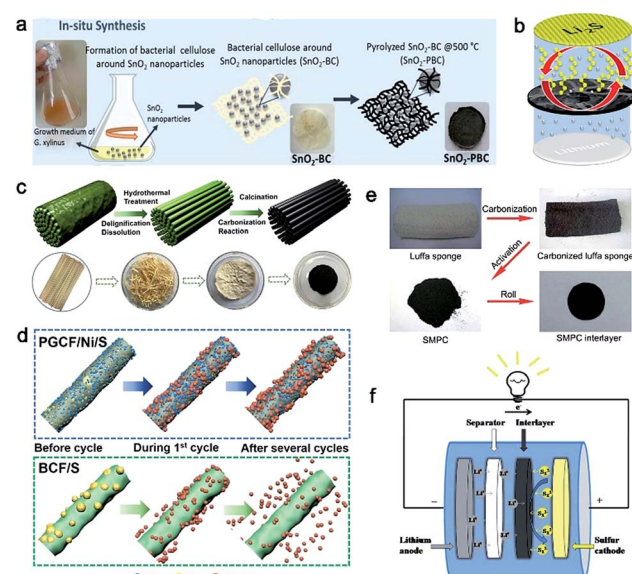


Fig. 5 (a) Fabrication process of SnO<sub>2</sub>-containing pyrolyzed bacterial cellulose (SnO<sub>2</sub>-PBC). (b) Schematic cell configuration of the Li-S battery with the SnO<sub>2</sub>-PBC interlayer. (a and b) Reproduced with permission.<sup>79</sup> Copyright 2018, Elsevier. (c) Schematic illustration of the mechanism of the PGCF/Ni/S and BCF/S cycling processes. (c and d) Reproduced with permission.<sup>82</sup> Copyright 2018, American Chemical Society. (e) The synthesis of the SMPC interlayer used in Li-S batteries. (f) Schematic cell configuration of the Li-S battery with the SMPC interlayer. (e and f) Reproduced with permission.<sup>83</sup> Copyright 2016, Royal Society of Chemistry.



carbonization at high temperature.<sup>83</sup> Unlike the aforementioned fiber-like materials, the obtained SMPC powder was rolled into a film using a twin roller and was punched into SMPC interlayers. The SMPC interlayer can prevent the shuttling of polysulfides toward the lithium metal anode. Such an interlayer opened up electron pathways to enable the reutilization of dissolved active materials during repeated discharge/charge processes (Fig. 5f).<sup>83</sup> Various interlayers derived from biomass for Li-S batteries have been compared and summarized in Table 2. Benefiting from the inherited cross-linked structures, rich heteroatom dopants, and simple fabrication processes of these bio-interlayers, the electrochemical performance of Li-S batteries has been significantly improved.

## 4 Binders derived from biomass for sulfur

The binder is a key component to keep electrode film integrity during the charge/discharge process. As a conventional binder,

polyvinylidene fluoride (PVDF) has been widely applied in the state-of-the-art LIBs. However, the high volume expansion of sulfur and the notorious shuttle effect challenge the effectiveness of PVDF in Li-S batteries. In addition, the requirement of using toxic and volatile *N*-methyl-2-pyrrolidone (NMP) as solvent for PVDF is also a concerning issue. Recently, several bio-polymers have been often reported derived from biomass for Li-S batteries with improved cycling stability.<sup>84</sup> Furthermore, the solvent for these bio-binders is water, having the merits of nontoxicity and low cost. In this section, the progress of bio-binders in Li-S batteries will be summarized.

Gum arabic (GA), a natural polymer derived from *Acacia senegal*, is mainly composed of highly branched polysaccharides, consisting of a galactan backbone chain with rich branched galactose, arabinose, rhamnose, and hydroxyproline side chains.<sup>26</sup> Due to the rich hydroxyl, carboxyl, and ether functional groups, the binding interaction between the polysulfides and GA can be effectively strengthened, which offers powerful assistance for improving sulfur utilization and cycle stabilization. Li *et al.* reported the application of GA as a binder

**Table 2** Categories, fabrication methods, structures and characteristics of interlayers derived from biomass

Source	Representative SEM/TEM image	Fabrication method	Surface chemical group
Bacterial cellulose <sup>78</sup>		Carbonization	Rich hydroxy
Cellulose paper <sup>81</sup>		Carbonization	Rich hydroxy
Bacterial cellulose <sup>79</sup>		Carbonization	SnO2 modification
Crab shell <sup>74</sup>		KOH activation	Rich hydroxy
Cotton <sup>52</sup>		Carbonization	Rich hydroxy
Lignin fibers <sup>85</sup>		Carbonization	Rich hydroxy
<i>Luffa</i> <sup>83</sup>		Carbonization	Sulfur dopants



for Li–S batteries.<sup>26</sup> The molecular structure of GA is revealed by Fourier transform infrared (FTIR) spectroscopy (Fig. 6a and b). The X-ray absorption spectroscopy (XAS) results (Fig. 6c) suggest that CA could chemically bond with polysulfides with no additional treatment, providing the direct mechanism for GA to suppress polysulfide dissolution in organic electrolytes. The sulfur cathode using the GA binder delivers a high initial capacity of  $1157 \text{ mA h g}^{-1}$  and a stable cycle life of more than 500 cycles at a current density of 0.2C.

Sodium-alginate (SA), a by-product derived from kelp or seaweed, has been widely used as a binder for LIBs due to its good adhesion and electrochemical stability. Zhang *et al.* reported on the preparation of sulfur cathodes using SA as the binder and water as the solvent for the first time.<sup>86</sup> As illustrated by FTIR spectroscopy (Fig. 6e), the decreased intensity of pyranose-ring deformation vibration peaks indicates strong chemical interaction between SA and sulfur powder. Such a resultant bonding is a critical factor that can stabilize the sulfur cathodes during cycling. In addition, compared with the PVDF binder, the SA binder endows the sulfur cathode with a much more porous structure (Fig. 6f and g), which was favourable for electrolyte permeation and thus fast lithium ion transfer. More importantly, the volume expansion of sulfur cathodes during the charge/discharge process could be effectively buffered due to the formation of porous-like sulfur cathodes.

Gelatin macromolecules were adopted as a typical water-soluble binder for Li–S batteries.<sup>87</sup> Biological gelatin has evident advantages in the preparation of sulfur cathodes. Firstly, as bio-polysulfides extracted from animal protein, rich ionizable groups such as COOH and NH<sub>2</sub> provide gelatin with great hydrophilic capability for trapping dissolved polysulfides. The substantial insolubility of gelatin in organic electrolytes (such as carbonic acid and ether) can keep the resultant sulfur cathodes integrated on the current collector. Secondly, as a widely used agent in the food, photographic and pharmaceutical industries, gelatin is easily scaled up. Huang *et al.* successfully employed gelatin as a binder in the design and

development of Li–S batteries.<sup>87,88</sup> Due to its high adhesion, strong dispersion, and stable electrochemistry, the sulfur cathodes using gelatin as the binder achieved a stable cycle life. Even at a high current density of  $1600 \text{ mA g}^{-1}$ , the sulfur cathodes based on the gelatin binder still display an evident discharge plateau, indicating that the sulfur in the cathode is converted to polysulfides.

Soy protein (SP) has abundant polar groups, such as amines and carboxyl groups, providing rich active sites for trapping dissolved polysulfides, which has been evidenced by density functional theory (DFT) calculation.<sup>89</sup> Meanwhile, the superior conductivity of SP promotes electrochemical reactions in sulfur

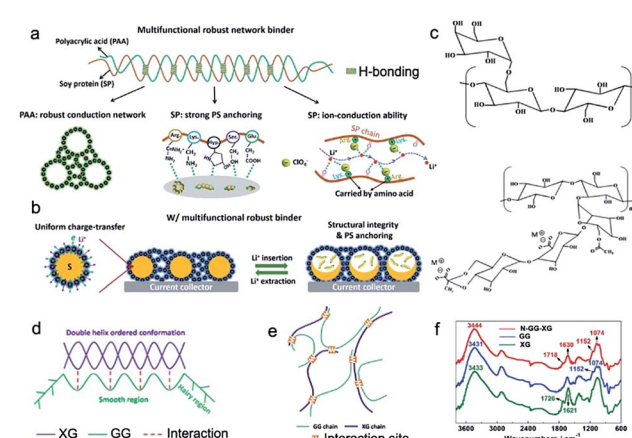


Fig. 7 (a) The schematic illustration of a robust and multi-functional binder (SP–PAA) via the incorporation of two bio-derived materials. (b) The structural changes of the obtained bio-derived binder in sulfur cathodes during discharge/charge processes. (a and b) Reproduced with permission.<sup>89</sup> Copyright 2019, Royal Society of Chemistry. (c) Chemical structures of bio-derived GG and XG. (d and e) Schematic of the chemical binding effect between GG and XG. (f) FTIR spectra of GG, XG and N-GG-XG. (c–f) Reproduced with permission.<sup>90</sup> Copyright 2017, Royal Society of Chemistry.

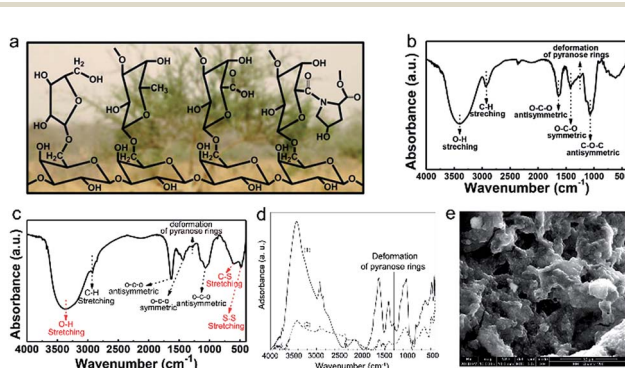


Fig. 6 (a) Chemical structure of GA with the background of *Acacia senegal*. (b) FTIR spectra of GA. (c) FTIR spectroscopy of a mixture of GA–polysulfide composites. (a–c) Reproduced with permission.<sup>26</sup> Copyright 2015, Wiley-VCH. (d) FTIR spectroscopy spectra of (1) Na-alginate and (2) Na-alginate sulfur electrodes. (e) SEM images of the Na-alginate sulfur cathode. (d and e) Reproduced with permission.<sup>86</sup> Copyright 2013, Elsevier.

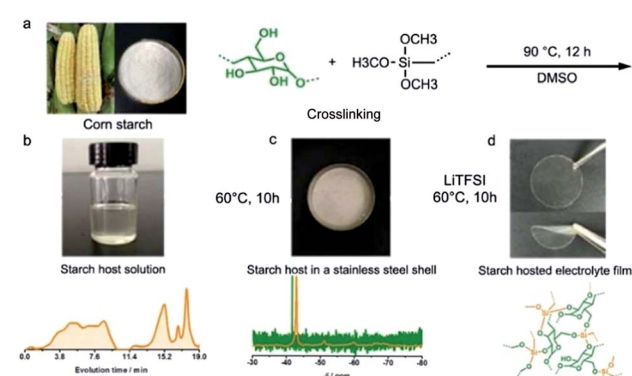


Fig. 8 (a) Schematic diagram of starch host synthesis. (b) The digital image of starch host solution using DMSO as solvent and the corresponding GPC result. (c) Solid state Si NMR spectrum of the starch host after vaporizing DMSO at  $60 \text{ }^\circ\text{C}$  for 10 h. (d) The digital image of the transparent and flexible electrolyte film and a suggested structure of the starch host. (a–d) Reproduced with permission.<sup>91</sup> Copyright 2016, Royal Society of Chemistry.



Table 3 The categories, structures and characteristics of bio-derived polymers as binders for Li–S batteries

Categories	Source	Chemical structure	Solvent
Gum arabic <sup>92</sup>	<i>Acacia senegal</i>	Rich -OH	Water
Na-alginate <sup>86</sup>	Sea grass	Rich -OH and -COOH	Water
Gelatin <sup>87</sup>	Animal protein	Rich -COOH and -NH <sub>2</sub>	Water
Caboxymethylcellulose <sup>93</sup>	Cellulose	Rich -OH and -COOH	Water
Guar gum and xanthan gum <sup>90</sup>	Endosperm and <i>Xanthomonas</i>	Rich -OH and C=O	Water
Soy protein and poly(acrylic acid) <sup>89</sup>	Soya	Rich -COOH and -NH <sub>2</sub>	Water

cathodes. Zhong *et al.* reported a SP-PAA binder instead of the PVDF binder for sulfur cathodes, buffering their large volume change (Fig. 7a). The stable cycle lifespan of the high-loading sulfur cathode is attributed to high mechanical strength, strong adsorption for polysulfides, and good ionic conductivity (Fig. 7b). In addition, the SP-PAA binder could effectively adjust the uniformity, the porous structure, and the interface in the resulting sulfur cathodes, which is beneficial for improving the coulombic efficiency. This strategy provides a facile method for stabilizing the cycle life of sulfur cathodes *via* using natural materials, indicating the great potential of biomass in Li–S batteries.

Exploring biopolymer binders should not be confined to the area of single biopolymers. Incorporation of various biopolymers offers a greater possibility. Well-designed sulfur cathodes with a 3D network binder are beneficial for dramatically improving the cycling stability of Li–S batteries. Liu *et al.* developed an adaptable binder for Li–S batteries using the intermolecular binding effect between guar gum (GG) and xanthan gum (XG) (Fig. 7c–e), which are, respectively, extracted from the endosperm of *Cyamopsis tetragonolobus* seeds and the bacterium *Xanthomonas campestris*.<sup>90</sup> Both GG and XG biopolymers are low-cost, non-toxic, and sustainable natural products (Fig. 7c). Due to the intermolecular binding effect between GG and XG (Fig. 7f), a binder network with rich oxygenous functional groups was obtained, providing strong adsorption for trapping dissolved polysulfides and realizing an ultrahigh areal specific capacity of 26.4 mA h cm<sup>−2</sup>. These results confirmed that high-energy-density Li–S batteries can be easily obtained using a biomass binder.

## 5 All-solid-state electrolyte derived from biomass for Li–S batteries

All-solid-state Li–S batteries with high energy density and high safety are a promising solution for next-generation energy storage systems.<sup>23</sup> However, the application of most reported all-solid-state electrolytes is limited by complicated procedures and high-cost chemicals. Hence, safer, cheaper and more sustainable solid-state electrolyte materials should be developed.<sup>80</sup>

Starch, a form of energy storage in plants, is composed of repeated glucose monomers with glycosidic linkages, which would allow reversible ion transfer. Hence, starch is used as an all-solid-state electrolyte for Li–S batteries. To enhance the stretchable properties of the electrolyte film,  $\gamma$ -(2,3-epoxypropoxy)propyltrimethoxysilane (KH560) was employed to

cross-link with the obtained corn starch.<sup>91</sup> As shown in Fig. 8a, the peak related to the chemical reaction between -OH groups from starch and -Si-(OCH<sub>3</sub>)<sub>3</sub> is observed (Fig. 8b). A possible structure of starch is composed of repeated glucose monomers joined by glycosidic linkages, which are described in detail in Fig. 8c and d. The highest ionic conductivity is achieved using 40 wt% bis(trifluoromethanesulfonimide) lithium salt (LiTFSI) and a 60 wt% starch-based biopolymer, whose optimized ratio of the obtained electrolyte film between starch and KH560 is 1 : 1. In addition, confirmed by a related electrochemical test, the as-prepared starch-based electrolyte can be compatible with high-voltage and high-capacity cathodes. The electrolyte is more economically and environmentally advantageous compared with other solid polymer electrolytes developed so far.

Table 3 displays the categories, structures, and characteristics of bio-derived polymers as binders or all-solid-state electrolytes for Li–S batteries. Different from the traditional PVDF binder using toxic NMP as the solvent, the bio-derived binders are more environment-friendly and cost-effective, and use water as the solvent. More importantly, due to the rich oxygen-containing groups such as -OH, -COOH, and C=O, these bio-derived polymers exhibit high adsorption ability for trapping polysulfides, which is beneficial for improving active sulfur utilization and stabilizing cycle life.

## 6 Conclusions and outlook

The past few years have witnessed the fast development of bio-derived materials for Li–S batteries due to their inherited structures and sustainability of chemical properties. In this review, we provided an overview of green biomass materials for Li–S batteries, highlighting various aspects toward the design and fabrication of sulfur hosts, separator membranes, binders, and all-solid-state electrolytes. A rich variety of carbon materials as sulfur hosts with various structures have been developed from various biomass materials using different fabrication strategies (Table 1), which provide plenty of building blocks for further development of Li–S battery commercialization.

Besides the application of biomass with specific structures, the activation step using KOH (or KHCO<sub>3</sub>, or NaCl, or ZnCl<sub>2</sub>, or KCO<sub>3</sub>, or H<sub>3</sub>PO<sub>4</sub>) is a flexible and applicable method for most biomass materials. A variety of bio-derived fiber materials such as BC, cellulose and cotton are built by simple methods to meet the specific applications as interlayer films in Li–S batteries (Table 2). With the help of rich oxygen-containing groups on the surface of bio-materials, the suppression of the shuttle effect



can be achieved with minimal cost. More importantly, instead of toxic NMP solvent, using water as the solvent for the bio-derived binder in Li-S batteries is more environmentally friendly and conducive to large-scale fabrication. Besides the successful development of biomass for a sulfur host and interlayer, bio-polymers extracted from biomass have also been applied in Li-S batteries as a binder (Table 3) or all-solid-state electrolyte. With the application of these natural bio-polymers, the employment of toxic and volatile organic solvents is under effective control.

Although the applications of bio-derived materials in Li-S batteries have obtained great progress, there are still several challenges for their commercialization in practical battery systems. At the end of this review, we attempt to propose several potential solutions to address these issues:

(1) The diversity of biomass ingredients endows the bio-derived sulfur host materials with chemical adsorption for trapping polysulfides, which is important for the improvement of sulfur utilization and cycle life. However, just relying on biomass itself will not satisfy the increasing requirement of high sulfur loading. The surface and interface modification using polar groups (*e.g.*, metal oxides, sulfides, and advanced polysulfides) for bio-derived sulfur hosts can be a promising strategy.

(2) Because of the microscopic size of most fiber-like biomaterials, the prepared interlayers show signs of weakness for trapping polysulfides in high sulfur loading cathodes. The whole size of the interlayer in sulfur cathodes is also not beneficial for promoting fast ion transfer. Therefore, developing an advanced bio-synthesis method is still urgently important, which can make bio-derived materials meet the ever-increasing demand for Li-S batteries. For example, the strategy of fabricating nanocellulose can reduce the size of micro-cellulose to the nanoscale, which can significantly improve its capability for trapping polysulfides.

(3) Low-cost bio-polymers as binders and electrolytes in sulfur cathodes made a great contribution to environmental protection. However, the extraction of some bio-polymers from biomass is very difficult, which raises the production cost. It is still hard to carry out large-scale fabrication of these bio-polymers with high quality and uniformity. Learning from the behavior of biomass, developing a bionic method may be a candidate approach to overcome this challenge. In summary, biomaterials are sustainable, earth abundant, low cost, biodegradable, and chemically accessible for modification. Due to these remarkable merits, the materials derived from biomass have been widely applied in Li-S batteries and achieved great progress. While various applications have been demonstrated, there are still some challenges such as large-scale fabrication in fundamental research and understanding to promote biomaterials toward commercial reality, especially for emerging applications, such as lithium metal anodes, catalysis, *etc.* In addition, in-depth research that can significantly improve the added value of biomaterials is also an area of concern. With a worldwide effort, new developments in Li-S batteries using biomaterials elaborated in this review will provide emerging technologies affecting our everyday life.

## Conflicts of interest

There are no conflicts to declare.

## Acknowledgements

H. Yuan and T. Liu contributed equally to this work. The authors acknowledge financial support by the National Natural Science Foundation of China (Grant no. 51722210, 51572240, U1802254, 51871201, and 51677170), and the Natural Science Foundation of Zhejiang Province (Grant no. LY16E070004 and LD18E020003).

## Notes and references

- 1 P. G. Bruce, S. A. Freunberger, L. J. Hardwick and J. M. Tarascon, *Nat. Mater.*, 2011, **11**, 19–29.
- 2 X. Ji, K. T. Lee and L. F. Nazar, *Nat. Mater.*, 2009, **8**, 500–506.
- 3 A. Manthiram, S. H. Chung and C. Zu, *Adv. Mater.*, 2015, **27**, 1980–2006.
- 4 X. Liu, J. Q. Huang, Q. Zhang and L. Mai, *Adv. Mater.*, 2017, **29**, 1601759.
- 5 H. Yuan, M. Wu, J. Zheng, Z. G. Chen, W. Zhang, J. Luo, C. Jin, O. Sheng, C. Liang, Y. Gan, Y. Xia, J. Zhang, H. Huang, Y. Liu, J. Nai and X. Tao, *Adv. Funct. Mater.*, 2019, **29**, 1809051.
- 6 Z. W. Seh, Y. Sun, Q. Zhang and Y. Cui, *Chem. Soc. Rev.*, 2016, **45**, 5605–5634.
- 7 O. Ogoke, G. Wu, X. Wang, A. Casimir, L. Ma, T. Wu and J. Lu, *J. Mater. Chem. A*, 2017, **5**, 448–469.
- 8 D.-W. Wang, Q. Zeng, G. Zhou, L. Yin, F. Li, H.-M. Cheng, I. R. Gentle and G. Q. M. Lu, *J. Mater. Chem. A*, 2013, **1**, 9382–9395.
- 9 H.-J. Peng, J.-Q. Huang, X.-B. Cheng and Q. Zhang, *Adv. Energy Mater.*, 2017, **7**, 1700260.
- 10 R. Fang, S. Zhao, Z. Sun, D. W. Wang, H. M. Cheng and F. Li, *Adv. Mater.*, 2017, **29**, 1606823.
- 11 Z. Li, J. Zhang, B. Guan, D. Wang, L. M. Liu and X. W. Lou, *Nat. Commun.*, 2016, **7**, 13065–13076.
- 12 X. Tao, J. Wang, C. Liu, H. Wang, H. Yao, G. Zheng, Z. W. Seh, Q. Cai, W. Li, G. Zhou, C. Zu and Y. Cui, *Nat. Commun.*, 2016, **7**, 11203–11212.
- 13 Z. W. Seh, J. H. Yu, W. Li, P. C. Hsu, H. Wang, Y. Sun, H. Yao, Q. Zhang and Y. Cui, *Nat. Commun.*, 2014, **5**, 5017.
- 14 G. Zhou, E. Paek, G. S. Hwang and A. Manthiram, *Adv. Energy Mater.*, 2016, **6**, 1501355.
- 15 Q. Pang, J. Tang, H. Huang, X. Liang, C. Hart, K. C. Tam and L. F. Nazar, *Adv. Mater.*, 2015, **27**, 6021–6028.
- 16 G. Zhou, E. Paek, G. S. Hwang and A. Manthiram, *Nat. Commun.*, 2015, **6**, 7760.
- 17 L. Sun, D. Wang, Y. Luo, K. Wang, W. Kong, Y. Wu, L. Zhang, K. Jiang, Q. Li, Y. Zhang, J. Wang and S. Fan, *ACS Nano*, 2016, **10**, 1300–1308.
- 18 S. Wang, H. Chen, J. Liao, Q. Sun, F. Zhao, J. Luo, X. Lin, X. Niu, M. Wu, R. Li and X. Sun, *ACS Energy Lett.*, 2019, **4**, 755–762.



19 H. Yao, G. Zheng, W. Li, M. T. McDowell, Z. Seh, N. Liu, Z. Lu and Y. Cui, *Nano Lett.*, 2013, **13**, 3385–3390.

20 J. Yoo, S. J. Cho, G. Y. Jung, S. H. Kim, K. H. Choi, J. H. Kim, C. K. Lee, S. K. Kwak and S. Y. Lee, *Nano Lett.*, 2016, **16**, 3292–3300.

21 D. Fang, Y. Wang, X. Liu, J. Yu, C. Qian, S. Chen, X. Wang and S. Zhang, *ACS Nano*, 2019, **13**, 1563–1573.

22 Y. Dong, S. Zheng, J. Qin, X. Zhao, H. Shi, X. Wang, J. Chen and Z. S. Wu, *ACS Nano*, 2018, **12**, 2381–2388.

23 X. Tao, Y. Liu, W. Liu, G. Zhou, J. Zhao, D. Lin, C. Zu, O. Sheng, W. Zhang, H. W. Lee and Y. Cui, *Nano Lett.*, 2017, **17**, 2967–2972.

24 S. Wang, Y. Ding, G. Zhou, G. Yu and A. Manthiram, *ACS Energy Lett.*, 2016, **1**, 1080–1085.

25 D. Dong, B. Zhou, Y. Sun, H. Zhang, G. Zhong, Q. Dong, F. Fu, H. Qian, Z. Lin, D. Lu, Y. Shen, J. Wu, L. Chen and H. Chen, *Nano Lett.*, 2019, **19**, 2343–2349.

26 G. Li, M. Ling, Y. Ye, Z. Li, J. Guo, Y. Yao, J. Zhu, Z. Lin and S. Zhang, *Adv. Energy Mater.*, 2015, **5**, 1500878.

27 Z. Yang, R. Li and Z. Deng, *ACS Appl. Mater. Interfaces*, 2018, **10**, 13519–13527.

28 X. Yu, G. Zhou and Y. Cui, *ACS Appl. Mater. Interfaces*, 2019, **11**, 3080–3086.

29 Z. W. Seh, H. Wang, P.-C. Hsu, Q. Zhang, W. Li, G. Zheng, H. Yao and Y. Cui, *Energy Environ. Sci.*, 2014, **7**, 672.

30 G. Zhou, L.-C. Yin, D.-W. Wang, L. Li, S. Pei, I. R. Gentle, F. Li and H.-M. Cheng, *ACS Nano*, 2013, **7**, 5367–5375.

31 G. Zheng, Q. Zhang, J. J. Cha, Y. Yang, W. Li, Z. W. Seh and Y. Cui, *Nano Lett.*, 2013, **13**, 1265–1270.

32 R. Chen, T. Zhao, J. Lu, F. Wu, L. Li, J. Chen, G. Tan, Y. Ye and K. Amine, *Nano Lett.*, 2013, **13**, 4642–4649.

33 H. J. Peng, J. Q. Huang and Q. Zhang, *Chem. Soc. Rev.*, 2017, **46**, 5237–5288.

34 J. Zhang, Y. Shi, Y. Ding, W. Zhang and G. Yu, *Nano Lett.*, 2016, **16**, 7276–7281.

35 X. Tao, J. Wang, Z. Ying, Q. Cai, G. Zheng, Y. Gan, H. Huang, Y. Xia, C. Liang, W. Zhang and Y. Cui, *Nano Lett.*, 2014, **14**, 5288–5294.

36 H. Yuan, X. Chen, G. Zhou, W. Zhang, J. Luo, H. Huang, Y. Gan, C. Liang, Y. Xia, J. Zhang, J. Wang and X. Tao, *ACS Energy Lett.*, 2017, **2**, 1711–1719.

37 Y. Cheng, S. Ji, X. Xu and J. Liu, *RSC Adv.*, 2015, **5**, 100089–100096.

38 J. Deng, M. Li and Y. Wang, *Green Chem.*, 2016, **18**, 4824–4854.

39 Y.-P. Gao, Z.-B. Zhai, K.-J. Huang and Y.-Y. Zhang, *New J. Chem.*, 2017, **41**, 11456–11470.

40 D. Liu, Q. Li, J. Hou and H. Zhao, *Sustainable Energy Fuels*, 2018, **2**, 2197–2205.

41 M. K. Rybarczyk, H.-J. Peng, C. Tang, M. Lieder, Q. Zhang and M.-M. Titirici, *Green Chem.*, 2016, **18**, 5169–5179.

42 J. Wang, P. Nie, B. Ding, S. Dong, X. Hao, H. Dou and X. Zhang, *J. Mater. Chem. A*, 2017, **5**, 2411–2428.

43 X. Yuan, B. Liu, J. Xu, X. Yang, K. Zeinu, X. He, L. Wu, J. Hu, J. Yang and J. Xie, *RSC Adv.*, 2017, **7**, 13595–13603.

44 L. Zhang, Y. Wang, B. Peng, W. Yu, H. Wang, T. Wang, B. Deng, L. Chai, K. Zhang and J. Wang, *Green Chem.*, 2014, **16**, 3926–3935.

45 J. Xu, K. Zhou, F. Chen, W. Chen, X. Wei, X.-W. Liu and J. Liu, *ACS Sustainable Chem. Eng.*, 2016, **4**, 666–670.

46 M. Wang, X. Xia, Y. Zhong, J. Wu, R. Xu, Z. Yao, D. Wang, W. Tang, X. Wang and J. Tu, *Chem.*, 2019, **25**, 3710–3725.

47 J. Zhang, Y. Cai, Q. Zhong, D. Lai and J. Yao, *Nanoscale*, 2015, **7**, 17791–17797.

48 Y. Xia, R. Fang, Z. Xiao, H. Huang, Y. Gan, R. Yan, X. Lu, C. Liang, J. Zhang, X. Tao and W. Zhang, *ACS Appl. Mater. Interfaces*, 2017, **9**, 23782–23791.

49 L. Xia, Y. Zhou, J. Ren, H. Wu, D. Lin, F. Xie, W. Jie, K. H. Lam, C. Xu and Q. Zheng, *Energy Fuels*, 2018, **32**, 9997–10007.

50 S. H. Chung, C. H. Chang and A. Manthiram, *ACS Nano*, 2016, **10**, 10462–10470.

51 X. Tao, J. Zhang, Y. Xia, H. Huang, J. Du, H. Xiao, W. Zhang and Y. Gan, *J. Mater. Chem. A*, 2014, **2**, 2290–2296.

52 B. Zheng, N. Li, J. Yang and J. Xi, *Chem. Commun.*, 2019, **55**, 2289–2292.

53 J. Zhou, Y. Guo, C. Liang, J. Yang, J. Wang and Y. Nuli, *Electrochim. Acta*, 2018, **273**, 127–135.

54 Y. Zhong, X. Xia, S. Deng, J. Zhan, R. Fang, Y. Xia, X. Wang, Q. Zhang and J. Tu, *Adv. Energy Mater.*, 2018, **8**, 1701110.

55 Y. Li, K. K. Fu, C. Chen, W. Luo, T. Gao, S. Xu, J. Dai, G. Pastel, Y. Wang, B. Liu, J. Song, Y. Chen, C. Yang and L. Hu, *ACS Nano*, 2017, **11**, 4801–4807.

56 C. Luo, H. Zhu, W. Luo, F. Shen, X. Fan, J. Dai, Y. Liang, C. Wang and L. Hu, *ACS Appl. Mater. Interfaces*, 2017, **9**, 14801–14807.

57 W. Wu, J. Pu, J. Wang, Z. Shen, H. Tang, Z. Deng, X. Tao, F. Pan and H. Zhang, *Adv. Energy Mater.*, 2018, **8**, 1702373.

58 J. Qu, S. Lv, X. Peng, S. Tian, J. Wang and F. Gao, *J. Alloys Compd.*, 2016, **671**, 17–23.

59 J. Li, F. Qin, L. Zhang, K. Zhang, Q. Li, Y. Lai, Z. Zhang and J. Fang, *J. Mater. Chem. A*, 2014, **2**, 13916.

60 Y. Xia, H. Zhong, R. Fang, C. Liang, Z. Xiao, H. Huang, Y. Gan, J. Zhang, X. Tao and W. Zhang, *J. Power Sources*, 2018, **378**, 73–80.

61 J. Han, X. Chen, B. Xi, H. Mao, J. Feng and S. Xiong, *ChemistrySelect*, 2018, **3**, 10175–10181.

62 M. Manoj, C. Muhammed Ashraf, M. Jasna, K. M. Anilkumar, B. Jinisha, V. S. Pradeep and S. Jayalekshmi, *J. Colloid Interface Sci.*, 2019, **535**, 287–299.

63 S. Zhang, M. Zheng, Z. Lin, N. Li, Y. Liu, B. Zhao, H. Pang, J. Cao, P. He and Y. Shi, *J. Mater. Chem. A*, 2014, **2**, 15889–15896.

64 Z. H. Chen, X. L. Du, J. B. He, F. Li, Y. Wang, Y. L. Li, B. Li and S. Xin, *ACS Appl. Mater. Interfaces*, 2017, **9**, 33855–33862.

65 C. Schneidermann, C. Kensy, P. Otto, S. Oswald, L. Giebel, D. Leistenschneider, S. Gratz, S. Dorfler, S. Kaskel and L. Borchardt, *ChemSusChem*, 2019, **12**, 310–319.

66 J. Liu, B. Liu, C. Wang, Z. Huang, L. Hu, X. Ke, L. Liu, Z. Shi and Z. Guo, *J. Alloys Compd.*, 2017, **718**, 373–378.

67 J. Zhang, J. Xiang, Z. Dong, Y. Liu, Y. Wu, C. Xu and G. Du, *Electrochim. Acta*, 2014, **116**, 146–151.



68 M. Zheng, Q. Hu, S. Zhang, H. Tang, L. Li and H. Pang, *Appl. Sci.*, 2017, **7**, 1036–1047.

69 L. Hencz, X. Gu, X. Zhou, W. Martens and S. Zhang, *J. Mater. Sci.*, 2017, **52**, 12336–12347.

70 Y. Zhao, L. Wang, L. Huang, M. Y. Maximov, M. Jin, Y. Zhang, X. Wang and G. Zhou, *Nanomaterials*, 2017, **7**, 402–412.

71 C. Hernández-Rentero, R. Córdoba, N. Moreno, A. Caballero, J. Morales, M. Olivares-Marín and V. Gómez-Serrano, *Nano Res.*, 2017, **11**, 89–100.

72 Y. Yan, M. Shi, Y. Wei, C. Zhao, M. Carnie, R. Yang and Y. Xu, *J. Alloys Compd.*, 2018, **738**, 16–24.

73 X.-l. You, L.-j. Liu, M.-y. Zhang, M. D. Walle, Y. Li and Y.-N. Liu, *Mater. Lett.*, 2018, **217**, 167–170.

74 H. Shao, F. Ai, W. Wang, H. Zhang, A. Wang, W. Feng and Y. Huang, *J. Mater. Chem. A*, 2017, **5**, 19892–19900.

75 T. Liu, X. Sun, S. Sun, Q. Niu, H. Liu, W. Song, F. Cao, X. Li, T. Ohsaka and J. Wu, *Electrochim. Acta*, 2019, **295**, 684–692.

76 Y. Huang, Z. Lin, M. Zheng, T. Wang, J. Yang, F. Yuan, X. Lu, L. Liu and D. Sun, *J. Power Sources*, 2016, **307**, 649–656.

77 S. Li, T. Mou, G. Ren, J. Warzywoda, Z. Wei, B. Wang and Z. Fan, *J. Mater. Chem. A*, 2017, **5**, 1650–1657.

78 Y. Huang, M. Zheng, Z. Lin, B. Zhao, S. Zhang, J. Yang, C. Zhu, H. Zhang, D. Sun and Y. Shi, *J. Mater. Chem. A*, 2015, **3**, 10910–10918.

79 K. B. Celik, E. C. Cengiz, T. Sar, B. Dursun, O. Ozturk, M. Y. Akbas and R. Demir-Cakan, *J. Colloid Interface Sci.*, 2018, **530**, 137–145.

80 A. Song, Y. Huang, X. Zhong, H. Cao, B. Liu, Y. Lin, M. Wang and X. Li, *J. Membr. Sci.*, 2018, **556**, 203–213.

81 S. Li, G. Ren, M. N. F. Hoque, Z. Dong, J. Warzywoda and Z. Fan, *Appl. Surf. Sci.*, 2017, **396**, 637–643.

82 X. Zhang, Y. Zhong, X. Xia, Y. Xia, D. Wang, C. Zhou, W. Tang, X. Wang, J. B. Wu and J. Tu, *ACS Appl. Mater. Interfaces*, 2018, **10**, 13598–13605.

83 J. Yang, F. Chen, C. Li, T. Bai, B. Long and X. Zhou, *J. Mater. Chem. A*, 2016, **4**, 14324–14333.

84 A. Ghosh, S. Shukla, G. S. Khosla, B. Lochab and S. Mitra, *Sci. Rep.*, 2016, **6**, 25207–25220.

85 T. Liu, S. Sun, W. Song, X. Sun, Q. Niu, H. Liu, T. Ohsaka and J. Wu, *J. Mater. Chem. A*, 2018, **6**, 23486–23494.

86 W. Bao, Z. Zhang, Y. Gan, X. Wang and J. Lia, *J. Energy Chem.*, 2013, **22**, 790–794.

87 Q. Wang, W. Wang, Y. Huang, F. Wang, H. Zhang, Z. Yu, A. Wang and K. Yuan, *J. Electrochem. Soc.*, 2011, **158**, A775–A779.

88 J. Sun, Y. Huang, W. Wang, Z. Yu, A. Wang and K. Yuan, *Electrochim. Acta*, 2008, **53**, 7084–7088.

89 X. Fu, L. Scudiero and W.-H. Zhong, *J. Mater. Chem. A*, 2019, **7**, 1835–1848.

90 J. Liu, D. G. D. Galpaya, L. Yan, M. Sun, Z. Lin, C. Yan, C. Liang and S. Zhang, *Energy Environ. Sci.*, 2017, **10**, 750–755.

91 Y. Lin, J. Li, K. Liu, Y. Liu, J. Liu and X. Wang, *Green Chem.*, 2016, **18**, 3796–3803.

92 S. Tu, X. Chen, X. Zhao, M. Cheng, P. Xiong, Y. He, Q. Zhang and Y. Xu, *Adv. Mater.*, 2018, **30**, e1804581.

93 L. Luo, S. H. Chung, H. Yaghoobnejad Asl and A. Manthiram, *Adv. Mater.*, 2018, **30**, e1804149.

